

Explore Faster Localization Learning For Scene Text Detection

Yuzhong Zhao¹, Yuanqiang Cai², Weijia Wu³, Weiqiang Wang^{1†}

Abstract

Generally pre-training and long-time training computation are necessary for obtaining a good-performance text detector based on deep networks. In this paper, we present a new scene text detection network (called FANet) with a Fast convergence speed and Accurate text localization. The proposed FANet is an end-to-end text detector based on transformer feature learning and normalized Fourier descriptor modeling, where the Fourier Descriptor Proposal Network and Iterative Text Decoding Network are designed to efficiently and accurately identify text proposals. Additionally, a Dense Matching Strategy and a well-designed loss function are also proposed for optimizing the network performance. Extensive experiments are carried out to demonstrate that the proposed FANet can achieve the SOTA performance with fewer training epochs and no pre-training. When we introduce additional data for pre-training, the proposed FANet can achieve SOTA performance on MSRA-TD500, CTW1500 and TotalText. The ablation experiments also verify the effectiveness of our contributions.

1. Introduction

Scene text detection is an important task of computer vision, and a basis of various text-related applications, so many researchers are concerned about the issue [34, 39, 14, 30, 28]. The rise and wide application of deep learning make great progress in scene text detection, so the best performance on benchmark datasets is refreshed constantly. However, most of the state-of-the-art methods [26, 18, 38, 8, 31, 29] rely on long-time training to achieve a good performance. Generally researchers use related large datasets for *long-time pre-training*, and then fine-tune the network on the target dataset, or directly carry out *long-time training* on the target dataset. These approaches are not suitable for scenarios that require to rapidly generate

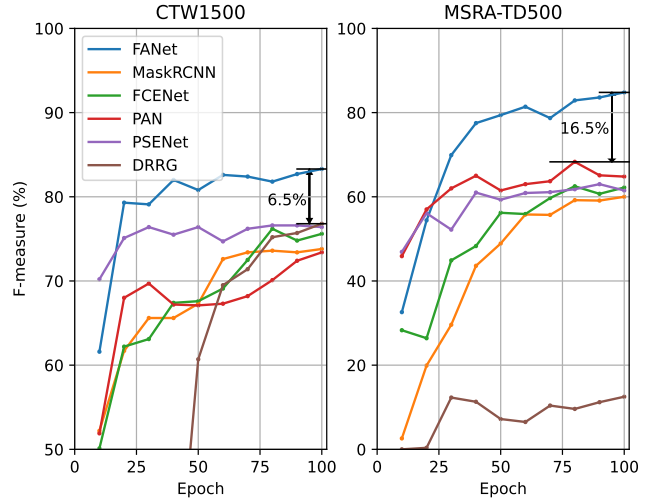


Figure 1 – The comparison of convergence performance between the proposed FANet and other state-of-the-art (SOTA) methods. After the training of 100 epochs, the FANet outperforms current best SOTA method by 6.5% (83.3%vs.76.8%) and 16.5% (84.8%vs.68.3%) based on F-measure on datasets CTW1500 and MSRA-TD500 respectively.

models or no large dataset for pre-training.

Inspired by the feature learning ability of the transformer [22] and deformable DETR[37] and the representation ability of Fourier descriptor for arbitrary contours [38], we present a scene text detection network (called FANet) with a Fast convergence speed and Accurate text localization, where the transformer is combined with Fourier descriptor to localize arbitrary-shaped text regions. The DETR based methods [1] can scale-invariantly localize the rectangular target regions. The Fourier descriptor proposed by [38] can model target regions of arbitrary contours, but it cannot be embedded into the DETR detection framework. Thus, we propose a normalization method for Fourier descriptor to enable the DETR based methods to predict the normalized text regions of arbitrary shape. However, we find that the established framework based on the proposed normalization method has slow convergence and low accuracy due to two aspects of reasons, i.e., (1) *the change of regression target* makes the deformable DETR component become sub-

¹ University of Chinese Academy of Sciences, China.

² Beijing University of Posts and Telecommunications, China.

³ Zhejiang University, China.

[†] Corresponding author. (wqwang@ucas.ac.cn)

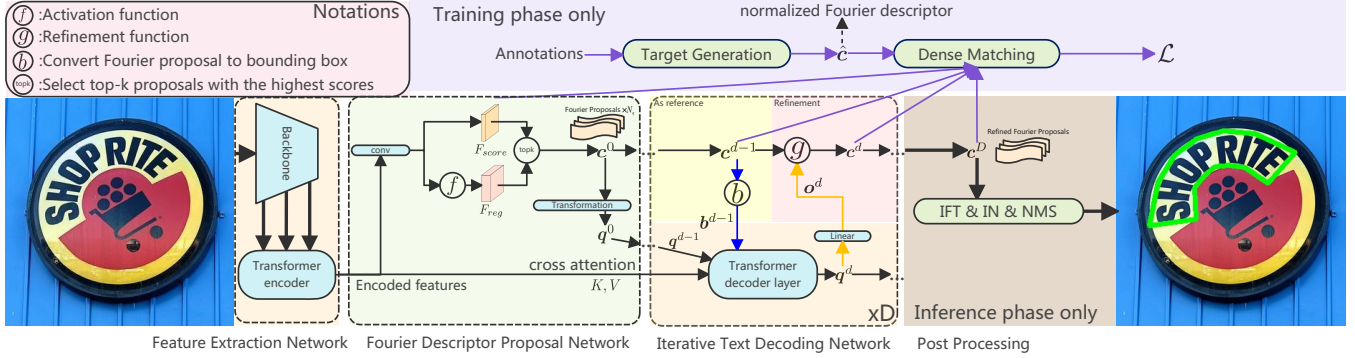


Figure 2 – Overview of the proposed FANet. c^d denotes the Fourier proposal predicted by d -th transformer decoder layer, q^{d-1} denote the input query for d -th transformer decoder layer, $d = 1, \dots, D$, where D is the number of decoder layers (6 in our experiments). As some special cases, c^0 denotes the Fourier proposal predicted by Fourier Descriptor Proposal Network (FDPN), q^D is the encoded memory of the last transformer decoder layer. We only describe the calculation process of a single proposal c^D in the network for simplicity. In the Iterative Text Decoding Network (ITDN), the blue top-down arrow indicates that the Fourier descriptor is used as the reference location for the Multi-Scale Deformable Attention module, the orange bottom-up arrow indicates that the offset predicted by the transformer decoder layer is used to refine the Fourier proposals.

optimal and (2) the *Hungarian Matching Strategy* hinders the rapid convergence of the network. Correspondingly, we first make some effective changes to the structure of deformable DETR. Concretely, we propose a Fourier Descriptor Proposal Network (FDPN) to get better candidates for the text decoder. Then, we build an Iterative Text Decoding Network (ITDN) to iteratively refine Fourier proposals. Finally, we propose a well-designed loss function to optimize the descriptor representations and calculate the matching cost. Additionally, we propose a Dense Matching Strategy (DMS) to greatly speed up the convergence and improve the detection accuracy within fewer training epochs. As shown in Figure 1, the proposed FANet can obtain an F-measure of 83.3% and 84.8% respectively, after training only 100 epochs on datasets CTW1500 [16] and MSRA-TD500 [33] without pre-training, which outperforms current best SOTA methods [35, 26] by 6.5% (83.3%vs.76.8%) and 16.5% (84.8%vs.68.3%) respectively. The main contributions of this paper are summarized as follows.

- We present a scene text detection network FANet with fast convergence speed and accurate localization, which uses the transformer to learn text features, and the normalized Fourier descriptor to represent text regions. The proposed FANet has achieved SOTA performances on multiple public benchmarks, *e.g.*, MSRA-TD500, CTW1500 and TotalText.
- We make many changes to the original deformable DETR, including Fourier Descriptor Proposal Network (FDPN), Iterative Text Decoding Network (ITDN) and well-designed loss function. These components can effectively improve the convergence speed and accuracy of FANet.
- We propose a Dense Matching Strategy (DMS), which

significantly improves the convergence speed and accuracy of FANet within fewer training epochs.

2. Related Works

2.1. Transformer modeling

The transformer [22] with both self-attention and cross-attention mechanism has achieved great success in both machine translation [6] and visual recognition [7]. For example, DETR [1] first adopts the transformer architecture for the object detection task. deformable DETR [37] extends DETR with a deformable attention module that reduces the training time significantly. Some previous works also try to explore the potential of transformer on text spotting task. Wu *et al.* [27, 32] proposed to track and spot text in video with transformer sequence modeling. [18] adopts the transformer architecture in multi-orientation text detection for the first time, but it still suffers from the problems of requiring massive data for pre-training, slow convergence, poor performance and inadequate representation ability. By using better contour representation, feature extraction and network optimization methods, we make the proposed FANet based on transformer surpasses the SOTA text detection algorithm based on CNNs [38, 4, 26].

2.2. Text Region Representation

Text regions can be modeled via per-pixel masks [25, 26], or modeled by parameters in specified representation spaces. For example, TextRay [24] represents the text contours in the polar system. ABCNet [15] introduced Bezier curves to parameterize curved texts. FCENet [38] represents the text instances in the Fourier domain, which allows to represent any closed continuous contour in robust and simple manners. In this paper, we further present a new normalized Fourier descriptor to represent the normalized

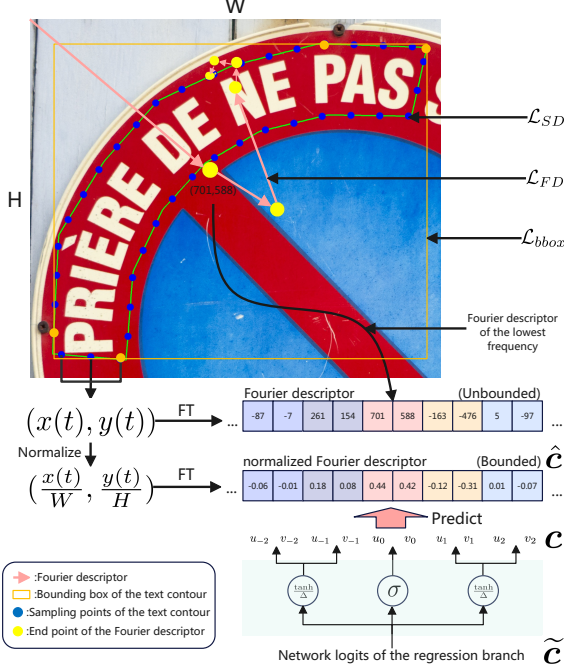


Figure 3 – Description of the Fourier descriptor normalization.

text regions of arbitrary shapes, which makes it possible to embed the text representation based on Fourier descriptor into the detection framework based on transformers.

3. Method Description

3.1. Overview

As shown in Figure 2, the proposed FANet mainly consists of three parts: Feature Extraction Network (FEN), Fourier Descriptor Proposal Network (FDPN) and Iterative Text Decoding Network (ITDN). For a given image, it is first encoded as features by the FEN, which consists of a backbone and a transformer encoder. The encoded features are then fed into the FDPN to obtain a set of arbitrary-shaped text contours represented as normalized Fourier descriptor and the object queries transformed from them. Further, the encoded features, the object queries and the N_q Fourier proposals with the highest scores are jointly fed into the ITDN to obtain the refined Fourier proposals, where N_q is the number of queries of the transformer decoder (300 in our experiments). Finally, we get the detection results after applying Inverse Fourier transform (IFT), Inverse Normalization (IN) and Non-Maximum Suppression (NMS) to the refined Fourier proposals.

3.2. Fourier Descriptor Normalization

Target generation. FCENet uses a complex-value function $z(t) = x(t) + iy(t)$, $t \in [0, 1]$ to represent a text contour, where $(x(t), y(t))$ denotes the spatial co-

ordinate of the text contour. To make the contour representation scale-invariant, we present a normalized form $\mathcal{Z}(t) = \frac{x(t)}{W} + i\frac{y(t)}{H} = \mathcal{X}(t) + i\mathcal{Y}(t)$, where H, W are the height and width of a given image. Since we cannot obtain the analytical form of text contour function \mathcal{Z} in real scenario, we can discretize the continual function \mathcal{Z} into N points, i.e., $\{\mathcal{Z}(\frac{n}{N})\}$, $n \in \{0, \dots, N-1\}$. Correspondingly, we can calculate the Fourier descriptor of a normalized text contour by Discrete Fourier Transform (DFT), i.e.,

$$\hat{c}_k = \frac{1}{N} \sum_{n=0}^{N-1} \mathcal{Z}(\frac{n}{N}) e^{-2\pi i k \frac{n}{N}}, k \in \Psi, \quad (1)$$

where $\hat{c}_k = \hat{u}_k + i\hat{v}_k \in \mathbb{C}$, \hat{u}_k and \hat{v}_k are real part and imaginary part of \hat{c}_k , $\Psi \triangleq \{-K, \dots, 0, \dots, K\}$, K is the highest frequency index reserved for the Fourier descriptor of the text contour ($K=5$ in our experiments). Thus, each ground-truth text contour can be represented as a normalized Fourier descriptor, $\hat{c} = [\hat{u}_{-K}, \hat{v}_{-K}, \dots, \hat{u}_0, \hat{v}_0, \dots, \hat{u}_K, \hat{v}_K] \in \mathbb{R}^{4K+2}$. We take normalized Fourier descriptor as regression targets. As shown in Figure 3, the values of original Fourier descriptor are generally large and unbounded, while the values of normalized Fourier descriptor all fall into a small region with fixed boundaries, i.e.,

$$(\hat{u}_0, \hat{v}_0) \in [0, 1]^2, \quad (2)$$

$$(\hat{u}_k, \hat{v}_k) \in [-\frac{2}{\pi}, \frac{2}{\pi}]^2, k \in \Psi, k \neq 0. \quad (3)$$

New activation function. Considering the above properties of normalized Fourier descriptor, the commonly used activation functions cannot meet our requirements. For example, the identity function is an unbounded function that does not fit the bounded regression target well. The sigmoid function σ cannot output negative values. The range of tanh is much larger than our regression target, which results in too many invalid predictions. So we define a new activation function $f(\tilde{c})$ suitable for the regression of proposed normalized Fourier descriptor as

$$c_i = f(\tilde{c}_i) = \begin{cases} \sigma(\tilde{c}_i) & i = 2K, 2K+1, \\ \frac{\tanh(\tilde{c}_i)}{\Delta} & i \in \Omega / \{2K, 2K+1\}, \end{cases} \quad (4)$$

where $\tilde{c} \in \mathbb{R}^{4K+2}$ is the stimulus, and $c \in \mathbb{R}^{4K+2}$ is the prediction of regression branches, where $\Omega = \{0, \dots, 4K+1\}$ is the index set aligned with Ψ , Δ is a hyperparameter that controls the output range of function $f(\tilde{c})$ and we set it to $\frac{\pi}{2}$ to best match the range of our regression target. As shown in Figure 3, we use the proposed activation function for the unbounded network logits of the regression branches where we need to predict the normalized Fourier descriptor by the networks, such as FDPN and ITDN.

3.3. Fourier Descriptor Proposal Network

We build a lightweight Fourier Descriptor Proposal Network (FDPN) following the Feature Extraction Network. As shown in Figure 2, through a single convolution module, we predict two feature maps, *i.e.*, $F_{score} \in \mathbb{R}^{B \times 2 \times h_f \times w_f}$, $F_{reg} \in \mathbb{R}^{B \times (4K+2) \times h_f \times w_f}$, where B is the batch size, h_f and w_f are the height and width of the feature map. Each pixel on the feature map is assigned as an object query, which directly predicts a normalized Fourier descriptor and a corresponding score, *i.e.*, a Fourier proposal. The top N_q Fourier proposals with the highest scores are selected, and we convert them into the initial queries of the ITDN through a transformation layer, which consists of a linear layer and a position encoding layer as described in deformable DETR [37]. Finally, the proposals and the queries are sent to the ITDN, and N_q is also the number of queries of the transformer decoder.

3.4. Iterative Text Decoding Network

As shown in Figure 2, Iterative Text Decoding Network (ITDN) is composed of D duplicate modules, each module is consist of a deformable transformer decoder layer and a refinement layer. We let each module refine the Fourier descriptor based on the prediction from the previous module and we select the output of the last module as the final predictions. The refinement target of FANet is the normalized Fourier descriptor while the refinement target of deformable DETR [37] is normalized bounding boxes. To adapt to this change of regression target, we make some effective changes for the transformer decoder layer as follows:

(1) **Take the Fourier descriptor as the reference location for the Multi-Scale Deformable Attention Module.** As shown in Figure 2, in the calculation process of d -th transformer decoder layer, we first calculate the bounding box $\mathbf{b}^{d-1} = (x, y, w, h) \in [0, 1]^4$ of the Fourier proposal \mathbf{c}^{d-1} through a function b . Then we use $((p_x + x)w, (p_y + y)h)$ instead of (p_x, p_y) as the sampling location for the Multi-Scale Deformable Attention (MSDeformAttn) module [37], where (p_x, p_y) are the sampling offset predicted by the MSDeformAttn module. Such modifications make the sampled locations of the MSDeformAttn module related to the center and size of previously predicted text contour.

(2) **Use multiplication based refinement instead of the original addition based refinement for the nondc component of Fourier descriptor.** As shown in Figure 2, the refinement function maps a proposal $\mathbf{c}^{d-1} \in \mathbb{R}^{4K+2}$ and an offset prediction $\mathbf{o}^d \in \mathbb{R}^{4K+2}$ to a new proposal $\mathbf{c}^d \in \mathbb{R}^{4K+2}$, which can be formulated as $\mathbf{c}_i^d = g(\mathbf{c}_i^{d-1}, \mathbf{o}_i^d)$, $i \in \Omega$, where \mathbf{c}^{d-1} and \mathbf{c}^d denote the prediction of the regression branch of $(d-1)$ -th and d -th transformer decoder layer (\mathbf{c}_0 denotes the proposal output by FDPN), \mathbf{o}^d is the offset prediction of the d -th transformer decoder layer. refinement

function used by deformable DETR is as follows:

$$\mathbf{c}_i^d = g_1(\mathbf{c}_i^{d-1}, \mathbf{o}_i^d) = f(f^{-1}(\mathbf{c}_i^{d-1}) + \mathbf{o}_i^d), i \in \Omega, \quad (5)$$

where f and f^{-1} are the activation function and its reverse function. We propose a new multiplication based refinement function for the nondc component of the normalized Fourier descriptor as

$$\mathbf{c}_i^d = g_2(\mathbf{c}_i^{d-1}, \mathbf{o}_i^d) = f(f^{-1}(\mathbf{c}_i^{d-1})e^{\mathbf{o}_i^d}), \\ i \in \Omega / \{2K, 2K + 1\}. \quad (6)$$

The reason why we use such refinement function are summarized. If we assume that \mathbf{o}^d close to $\vec{0}$, which is reasonable because \mathbf{o}^d is the residual term of the prediction. Based on this assumption, we can prove that for the refinement function based on addition, we have

$$\lim_{\mathbf{o}_i^d \rightarrow 0} \left| \frac{\partial g_1}{\partial \mathbf{o}_i^d} \right| = \left| \frac{\partial f(z)}{\partial z} \Big|_{z=f^{-1}(\mathbf{c}_i^{d-1})} \right|, i \in \Omega, \quad (7)$$

and for the refinement function based on multiplication, we have

$$\lim_{\mathbf{o}_i^d \rightarrow 0} \left| \frac{\partial g_2}{\partial \mathbf{o}_i^d} \right| = \left| \frac{\partial f(z)}{\partial z} \Big|_{z=f^{-1}(\mathbf{c}_i^{d-1})} \right| |f^{-1}(\mathbf{c}_i^{d-1})|, \\ i \in \Omega / \{2K, 2K + 1\}. \quad (8)$$

As we can see, when calculating the gradient of \mathbf{o}_i^d , our multiplication based refinement function has an extra $|f^{-1}(\mathbf{c}_i^{d-1})|$ term compared with the original definition. It is easy to prove that the function $|f^{-1}(x)|$ is a monotonically increasing function of $|x|$ when f is σ or \tanh . We can deduce that $|f^{-1}(\mathbf{c}_i^{d-1})|$ term can adaptively increase the gradient of the Fourier descriptor if $|\mathbf{c}_i^{d-1}|$ becomes larger. This weighting scheme is intuitive and effective, because the numerically larger Fourier descriptor generally plays a leading role in the construction of the target contour, which means they should occupy a larger gradient in back propagation than others. As a special case, we still use the refinement function based on addition for the dc component (u_0, v_0) of Fourier descriptor. (u_0, v_0) is the center coordinate of the text contour and the optimization of the center coordinate of different targets should not be weighted by the absolute value of their position. In the ITDN, the refinement function is defined as

$$g(\mathbf{c}_i^d) = \begin{cases} g_1(\mathbf{c}_i^{d-1}, \mathbf{o}_i^d) & i = 2K, 2K + 1, \\ g_2(\mathbf{c}_i^{d-1}, \mathbf{o}_i^d) & i \in \Omega / \{2K, 2K + 1\}. \end{cases} \quad (9)$$

3.5. Optimization strategies

Dense Matching Strategy. The traditional Hungarian Matching Strategy (HMS) used in [21, 1, 37] only matches

one query for each ground-truth text instance, which we find is one of the causes of slow convergence of the network. The number of text instances in an image is usually limited, and we denote it as N_g . N_g is usually much less than the number of queries of the network N_q (300 in our experiments), *i.e.*, $N_g \ll N_q$. Using HMS means that only N_g queries are used as positive samples for the training of regression branch in each iteration, which makes the network easy to overfit and damages the performance of the network due to lack of positive samples. We propose to match multiple queries for each ground-truth text instance. Dense Matching Strategy (DMS) can effectively alleviate the problem of slow convergence, especially in the early stage of training. Since the DMS makes the FANet output overlapping detection results, we have to use the NMS as post-processing. Due to the small number of queries of DETR based methods and small number of N_m , the number of predictions is generally small, so the NMS only brings a low cost. The pseudo code of Dense Matching Strategy is summarized:

Algorithm 1 Dense Matching Strategy

Input:

$\hat{\mathcal{A}}$: a set of ground-truth text contours in a given image.

\mathcal{A} : a set of predict text contours in the image.

Parameter:

Cost : the cost function of the proposed FANet.

N_m : the number of predicted text contour matched for each ground truth text contour.

Output:

\mathcal{P} : a set of positive samples.

\mathcal{N} : a set of negtive samples.

```

1:  $\mathcal{P} \leftarrow \emptyset$ 
2:  $\hat{a} = |\hat{\mathcal{A}}|$ 
3:  $a = |\mathcal{A}|$ 
4:  $i = 1$ 
5:  $cost = \text{Cost}(\mathcal{A}, \hat{\mathcal{A}}) \in \mathbb{R}^{a \times \hat{a}}$ 
6: while  $i \leq N_m$  do
7:    $k, l = \text{Hungarian\_matcher}(cost)$ 
8:    $\mathcal{P} \leftarrow \mathcal{A}[k]$ 
9:    $cost[k, :] = +\infty$ 
10:   $i = i + 1$ 
11: end while
12:  $\mathcal{N} = \mathcal{A} - \mathcal{P}$ 
13: return  $\mathcal{P}, \mathcal{N}$ 

```

To use the DMS algorithm, we need to define a Cost function that takes the set of predicted text contours \mathcal{A} and the set of ground-truth text contours $\hat{\mathcal{A}}$ as input and outputs the cost between any two elements in the two sets. We use $\mathcal{C}_{cls} + \lambda \mathcal{C}_{reg}$ as the matching cost for any (c, \hat{c}) pair in the two sets, where $\mathcal{C}_{cls} = -\log(s)$, where s is the predicted text confidence score corresponding to proposal c , λ is the hyperparameter that balance the costs. We define \mathcal{C}_{reg} as

follows:

$$\mathcal{C}_{reg}(c, \hat{c}) = \mathcal{L}_{SD}(c, \hat{c}) + \alpha_1 \mathcal{L}_{FD}(c, \hat{c}) + \alpha_2 \mathcal{L}_{bbox}(c, \hat{c}), \quad (10)$$

$$\mathcal{L}_{SD}(c, \hat{c}) = \text{L1}[\mathcal{F}^{-1}(c), \mathcal{F}^{-1}(\hat{c})], \quad (11)$$

$$\mathcal{L}_{FD}(c, \hat{c}) = \text{L1}(c, \hat{c}), \quad (12)$$

$$\mathcal{L}_{bbox}(c, \hat{c}) = \text{GIOU}[b(c), b(\hat{c})]. \quad (13)$$

Where α_1, α_2 are the hyperparameters that balance the three matching costs. L1 is the L1 loss function, b is a function that convert Fourier proposal to bounding box, GIOU is the GIOU loss in [19], \mathcal{F}^{-1} is the Inverse Discrete Fourier Transform. For a given image, we first calculate the *cost* between \mathcal{A} and $\hat{\mathcal{A}}$, then we iteratively perform Hungarian Matching (HM) for N_m times. Each time we first add the proposals that match any ground-truth text contour to the positive sample set \mathcal{P} and then remove these proposals from the matching queue by setting the matched rows of *cost* to $+\infty$ to avoid repeated matching. Finally, we collect all the matched proposals as positive samples and the unmatched proposals as negative samples.

Loss function. The loss function of the proposed network is given by

$$\mathcal{L} = \mathcal{L}_{cls,0} + \lambda \mathcal{L}_{reg,0} + \sum_{i=1}^D w_i (\mathcal{L}_{cls,i} + \lambda \mathcal{L}_{reg,i}), \quad (14)$$

where $\mathcal{L}_{cls,0}$ and $\mathcal{L}_{reg,0}$ denote the classification and regression loss of the FDPN respectively, $\mathcal{L}_{cls,i}$ and $\mathcal{L}_{reg,i}$ denote the classification and regression loss of the i -th decoder layer, w_i is the hyperparameter that balance the losses of different transformer decoder layers, D is the number of decoder layers. We use focal loss [13] as our default classification loss for $\mathcal{L}_{cls,i}, i = 0, 1, \dots, D$. We define $\mathcal{L}_{reg,i}$ as follows:

$$\mathcal{L}_{reg,i} = \frac{1}{|\mathcal{M}_i|} \sum_{(c, \hat{c}) \in \mathcal{M}_i} (\mathcal{L}_{SD} + \alpha_1 \mathcal{L}_{FD} + \alpha_2 \mathcal{L}_{bbox}), \quad (15)$$

where $\mathcal{M}_i, i = 0, 1, \dots, d$ are the set of matched Fourier descriptor pairs of i -th decoder layer, *i.e.*, $\forall (c, \hat{c}) \in \mathcal{M}_i, c \in \mathcal{P}_i$, where \mathcal{P}_i is the positive sample set obtained by DMS at the i -th decoding layer.

4. Experiment

4.1. Implementation details

The backbone of FANet is ResNet-50 [9] which is pre-trained on ImageNet [5]. Following FCENet [38], during the target generation stage, we sample equidistantly a fixed number N ($N = 400$ in our experiments) points on the

Methods	Venue	Backbone	Ext.	ICDAR2015			MSRA-TD500			CTW1500			TotalText		
				R(%)	P(%)	F(%)	R(%)	P(%)	F(%)	R(%)	P(%)	F(%)	R(%)	P(%)	F(%)
TextSnake [17]	ECCV'18	VGG16 [20]	✓	80.4	84.9	82.6	73.9	83.2	78.3	85.3	67.9	75.6	74.5	82.7	78.4
PAN [26]	ICCV'19		✓	81.9	84.0	82.9	83.8	84.4	84.1	81.2	86.4	83.7	81.0	89.3	85.0
DB [12]	AAAI'20	Res50-DCN [3]	✓	83.2	91.8	87.3	79.2	91.5	84.9	80.2	86.9	83.4	82.5	87.1	84.7
CRNet [36]	MM'20		✓	84.5	88.3	86.4	82.0	86.0	84.0	80.9	87.0	83.8	82.5	85.8	84.1
[18]	CVPRW'21		✓	78.3	89.8	83.7	83.8	90.9	87.2	-	-	-	-	-	-
DRRG [35]	CVPR'20		✓	84.7	88.5	86.6	82.3	88.1	85.1	83.0	85.9	84.5	84.9	86.5	85.7
PCR [4]	CVPR'21	DLA34 [4]	✓	-	-	-	83.5	90.8	87.0	82.3	87.2	84.7	82.0	88.5	85.2
PSENet [25]	CVPR'19			79.7	81.5	80.6	-	-	-	75.6	80.6	78.0	75.1	81.8	78.3
PAN [26]	ICCV'19			77.8	82.9	80.3	77.3	80.7	78.9	77.7	84.6	81.0	79.4	88.0	83.5
TextRay [24]	MM'20			-	-	-	-	-	-	80.4	82.8	81.6	77.9	83.5	80.6
PCR [4]	CVPR'21			-	-	-	77.8	87.6	82.4	79.8	85.3	82.4	80.2	86.1	83.1
FCENet [38]	CVPR'21			84.2	85.1	84.6	-	-	-	80.7	85.7	83.1	79.8	87.4	83.4
FANet				83.8	85.6	84.7	83.3	91.7	87.3	84.3	85.6	84.9	83.3	86.2	84.8
FANet			✓	87.6	85.0	86.3	84.2	92.1	88.0	84.0	87.8	85.9	84.7	87.1	85.9

Table 1 – Comparison with recent state-of-the-art methods on ICDAR 2015, MSRA-TD500, CTW1500 and TotalText under the protocol of IoU@0.5, where 'Ext.' denotes extra training data. We use ResNet50 as the default backbone for our proposed FANet and all the compared algorithms.

Methods	ICDAR2015			MSRA-TD500			CTW1500			TotalText		
	30e	100e	500e	30e	100e	500e	30e	100e	500e	30e	100e	500e
PAN [26]	62.3	73.8	74.9	61.4	65.1	70.0	72.0	73.4	74.6	66.9	73.7	76.0
FCENet [38]	65.6	78.5	83.5	47.2	62.2	74.2	65.5	75.6	81.0	71.3	80.2	83.0
FANet†	73.9	82.6	83.5	62.1	70.6	83.5	75.6	81.2	84.6	79.0	81.2	84.6
FANet	77.2	84.1	84.7	70.7	84.8	87.3	79.1	83.3	84.9	81.9	84.1	84.8

Table 2 – Convergence performance comparison with recent state-of-the-art methods. We use F-measure as the evaluation protocol, and $\{30, 100, 500\}e$ means training $\{30, 100, 500\}$ epochs on the dataset. The results of other algorithms are reproduced in open-mocr [11]. † denote using original Hungarian Matching Strategy (HMS).

text contour, obtaining the resampled point sequence, i.e., $\{\mathcal{Z}(\frac{n}{N})\}$, $n \in \{0, \dots, N-1\}$. Then, we transform the resampled point sequence into its corresponding normalized Fourier descriptor with Equation 1. We set the highest level reserved for the Fourier descriptor K to 5. The number of queries of the transformer decoder N_q to 300. The number of transformer layers D to 6. For the hyperparameters that balance the losses, we set $[\lambda, \alpha_1, \alpha_2]$ equals to $[0.25, 5, 0.4]$ and set w_d to 1, $d = 1, 2, \dots, D$.

Optimization Setting. The experiments are conducted on the workstation with 8 Tesla V100 GPU. The data augmentation contains color jitter, random rotation, random horizontal flip, random scale, random crop, and random resize. Following the common practices, we ignore the blurred text regions labeled as “DO NOT CARE” during training. The network is trained using an Adam optimizer with the weight decay ratio equals to 0.0001 and we fix the batch size to 16. We use **poly** as our default learning rate policy, and we set its power as 0.9. For the experiments without pre-training, we set the match number of the DMS N_m to 3 by default and MSRA-TD500 to 10 and train the proposed FANet for 500 epochs separately on the dataset we report the results. For the experiment with pre-training, we first pre-trained our model for 25 epochs on COCO-

Textv2 [23], and then finetune our model for 250 epochs on the benchmark datasets respectively. we use HMS as default and DMS N_m to 5 for MSRA-TD500 by default when FANet is pretrained use COCOTextv2. For the convergence experiments in Table 2, as the learning rate attenuation strategy will damage the performance of the algorithm under the restriction of very little iterations, we keep the initial learning rate unchanged for the experiments of training 30 epochs. For the experiments of training more than 30 epochs, we keep the optimization settings of the re-implemented algorithms consistent with the original paper.

Inference setting. In the inference stage, we resize the long dimension of test images to 1080, 1280, 2200 and 1312 for MSRA-TD500, CTW1500, ICDAR2015 and TotalText respectively.

4.2. Comparison with the state-of-the-art methods

We evaluate the proposed FANet on four public benchmark datasets, i.e., ICDAR2015 [10], MSRA-TD500 [33], CTW1500 [16] and TotalText [2], and the experiments results are summarized in Table 1.

ICDAR2015. The proposed FANet achieves comparable performance with SOTA methods on ICDAR2015. It’s worth noting that the proposed FANet outperforms the pre-

vious DETR based text detection algorithm [18] by 2.6% (86.3% vs. 83.7%) based on F-measure with pre-training.

MSRA-TD500. The proposed FANet achieves the SOTA performance on MSRA-TD500. Specifically, if compared with the methods without pre-training, the proposed FANet outperforms the previous SOTA method PCR by 4.9% (87.3% vs. 82.4%) in F-measure. If compared with the algorithm with pre-training, the proposed FANet can still outperforms the previous SOTA method [18] by 0.8% (88.0% vs. 87.2%).

CTW1500. The proposed FANet achieves the SOTA performance on CTW1500. If compared with the methods without pre-training, the proposed FANet outperforms the previous SOTA method FCENet by 1.8% (84.9% vs. 83.1%) in F-measure. If compared with the algorithm with pre-training, the proposed FANet can still outperforms the previous SOTA method [4] by 1.2% (85.9% vs. 84.7%).

TotalText. The proposed FANet achieves the SOTA performance on TotalText. If compared with the methods without pre-training, the proposed FANet outperforms the previous SOTA method PAN by 1.3% (84.8% vs. 83.5%) in F-measure. If compared with the algorithm with pre-training, the proposed FANet can still outperforms the previous SOTA method [35] by 0.2% (85.9% vs. 85.7%).

Convergence Performance. Under the constraint of limited epochs, the proposed FANet can still achieve good results. In particular, with only 30 epochs of training, FANet surpass FCENet by 11.6%, 23.5%, 13.6%, 10.6%, surpass PAN by 14.9%, 9.3%, 7.1%, 15.0% based on F-measure on ICDAR2015, MSRA-TD500, CTW1500 and TotalText respectively, which shows that the proposed FANet can achieve much better performance than the previous SOTA methods with fewer epochs. With only 100 epochs of training, FANet can achieve the detection performance of 84.8% on MSRA-TD500, 83.3% on CTW1500 and 84.1% on TotalText, which already have achieved the SOTA performance if only compared with the methods without pre-training. In other words, we only need to train FANet on a server with 8 Tesla V100 for about 20 minutes, and we can get a SOTA text detector that achieve 84.8% F-measure on MSRA-TD500.

Qualitative Results. Some detection results of the proposed FANet are shown in Figure 4. For the datasets whose text instances are all rectangular boxes, we take the minimum enclosing rectangle for the text contour. As we can see, FANet is capable of detecting text in a variety of scenarios, including extremely long text in MSRA-TD500, scene text in ICDAR2015, curved text in CTW1500 and TotalText. Qualitative and quantitative results show that the proposed FANet has a wide range of application scenarios.

ITDN	FDPN	DMS	CTW1500			MSRA-TD500		
			R(%)	P(%)	F(%)	R(%)	P(%)	F(%)
			78.9	82.0	80.4	19.1	9.2	12.4
✓			79.2	87.4	83.1	58.8	67.7	62.9
✓	✓		82.5	86.9	84.6	79.2	88.3	83.5
✓	✓	✓	84.3	85.6	84.9	83.3	91.7	87.3

Table 3 – Ablation experiments on our proposed core components.

AF	NT	CTW1500			MSRA-TD500		
		R(%)	P(%)	F(%)	R(%)	P(%)	F(%)
identity		0.0	0.0	0.0	0.0	0.0	0.0
identity	✓	—	—	—	—	—	—
σ	✓	0.0	0.0	0.0	1.6	1.9	1.7
tanh	✓	82.9	85.7	84.3	75.8	86.6	80.8
ours	✓	82.5	86.9	84.6	79.2	88.3	83.5

Table 4 – Comparison between our activation function and other commonly used activation functions. AF denotes Activation Function and NT denotes whether to use the Normalized Fourier Descriptor as the regression target. "—" denotes that the network becomes untrainable and no result can be obtained.

4.3. Ablation study

We conduct ablation studies on CTW1500 and MSRA-TD500 under the protocol of IoU@0.5. We fix the number of training epochs for all experiments to 500 epochs.

Baseline and core components. Based on deformable DETR, we directly use normalized Fourier descriptor to replace bounding box as the regression target to obtain our baseline algorithm. As shown in Table 3, the baseline of the proposed method reaches 80.4% on CTW1500 and 12.4% on MSRA-TD500. Compared with our baseline, ITDN can bring relative improvements of 2.7% (83.1% vs. 80.4%) and 50.5% (62.9% vs. 12.4%) on CTW1500 and MSRA-TD500 respectively. Then, the addition of FDPN can bring relative improvements of 1.5% (84.6% vs. 83.1%) and 20.6% (83.5% vs. 62.9%) on CTW1500 and MSRA-TD500 respectively. Finally, the DMS can bring relative improvements of 0.3% (84.9% vs. 84.6%) and 3.8% (87.3% vs. 83.5%) on CTW1500 and MSRA-TD500 respectively. The above modules and strategies can significantly improve the performance of the network, especially for MSRA-TD500 which only has small number of training data.

Activation function. As shown in Figure 5, we first compare the performance between the normalized Fourier descriptor and the original Fourier descriptor when DETR like architecture is used. The network does not locate text well when the original Fourier descriptor is used which means that the original Fourier descriptor do not fit with DETR like detection architecture. As shown in line 2 of Table 4, the network will not be trainable if the activation function in the proposed FANet is replaced by identity function. Then we replace the activation function in the pro-

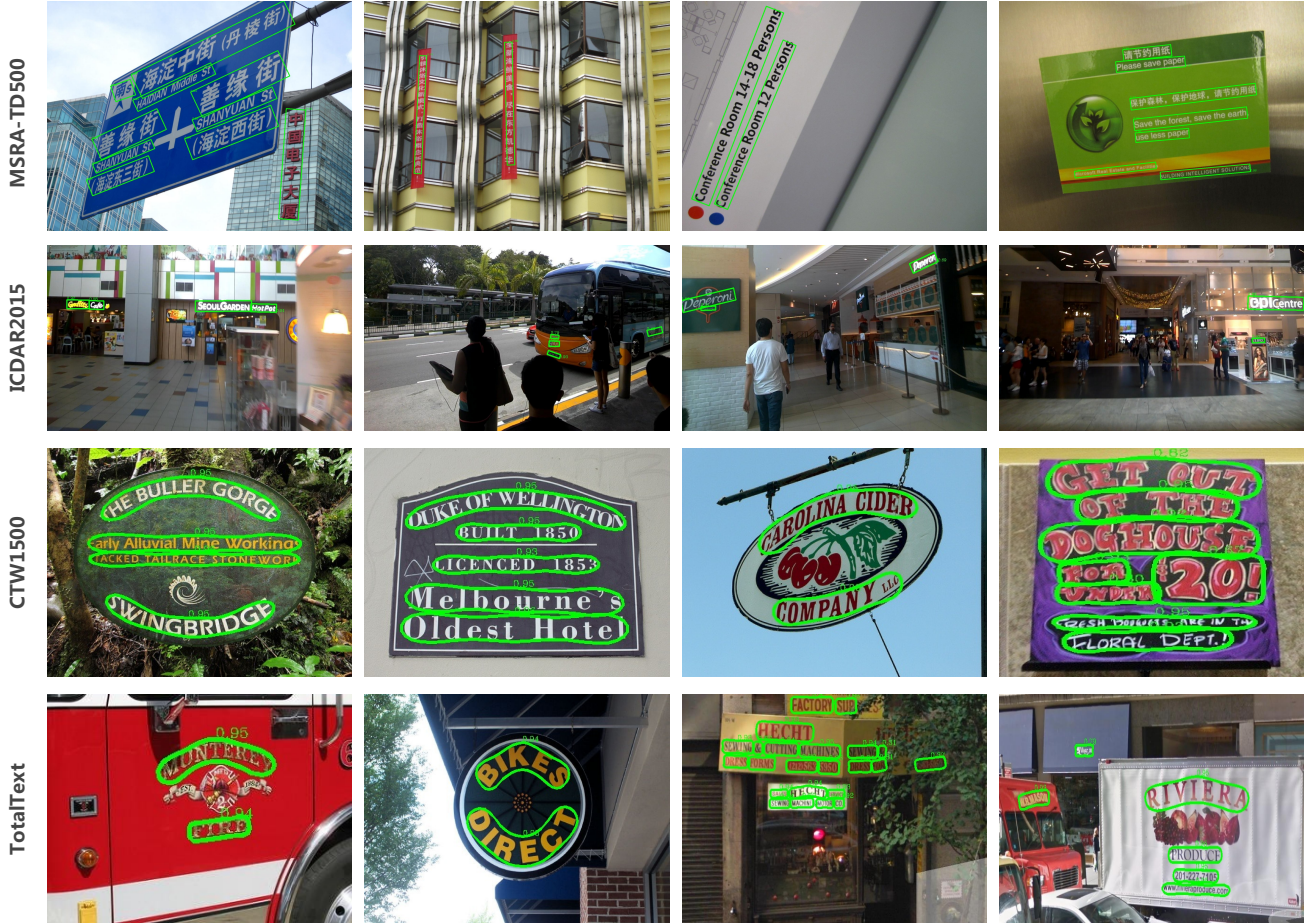


Figure 4 – Some detection results of our proposed method on MSRA-TD500, ICDAR2015, CTW1500 and TotalText.



Figure 5 – Comparison between normalized Fourier Descriptor regression target and original Fourier Descriptor regression target when DETR like detection architecture is used. (a) denotes using normalized Fourier Descriptor as regression target and our activation function, (b) denotes using original Fourier Descriptor as regression target and identity activation function like FCENet.

posed FANet with σ in line 3 of Table 4, which makes the detection performance decrease to a very low level, since the range of σ can not completely cover the normalized Fourier descriptor to be predicted. Finally, we test the performance when replacing the activation function by tanh in

line 4 of Table 4, which makes the corresponding F-measure of the network decrease by 0.3% (84.6% vs. 84.3%) and 2.7% (83.5% vs. 80.8%) on CTW1500 and MSRA-TD500 respectively. The experimental results show that it is more appropriate to use the activation function which can well match the range of regression target.

Iterative Text Decoding Network. As shown in Table 6, replacing the refinement function by the refinement function based on addition or multiplication can result in the decrease of F-measure for the proposed FANet by 1.9% and 1.1% on CTW1500, and by 22.0% and 5.9% on MSRA-TD500 respectively, this shows that the proposed refinement module is more suitable for the normalized Fourier descriptor. Not taking the Fourier descriptor as the reference location for the Multi-Scale Deformable Attention module reduce the F-measure performance of the proposed FANet by 5.0% and 21.2% on CTW1500 and MSRA-TD500 respectively, which shows that aggregating features near the text region is conducive to the accurate regression of the network to the text instances.

Loss function. As shown in Table 7, removing \mathcal{L}_{SD} ,

Match number	MSRA-TD500			ICDAR2015			CTW1500			TotalText		
	R(%)	P(%)	F(%)	R(%)	P(%)	F(%)	R(%)	P(%)	F(%)	R(%)	P(%)	F(%)
1	79.2	88.3	83.5	79.9	87.4	83.5	82.5	86.9	84.6	82.4	87.0	84.6
3	-	-	-	83.8	85.6	84.7	84.3	85.6	84.9	83.3	86.2	84.8
5	83.2	88.8	85.9	-	-	-	-	-	-	81.5	87.2	84.3
10	83.3	91.7	87.3	78.1	85.6	81.7	80.3	88.7	84.3	73.1	84.9	78.6
15	82.3	90.2	86.1	-	-	-	-	-	-	-	-	-

Table 5 – The impact of the match number of the Dense matching Strategy for the performance of the network under the restriction of training 500 epochs.

Refinement module	CTW1500			MSRA-TD500		
	R(%)	P(%)	F(%)	R(%)	P(%)	F(%)
w/o refinement	78.9	82.0	80.4	19.1	9.2	12.4
w/o reference	76.4	79.9	78.1	40.2	43.3	41.7
add	77.7	85.0	81.2	36.1	47.3	40.9
mul	78.8	85.4	82.0	50.3	65.7	57.0
ours	79.2	87.4	83.1	58.8	67.7	62.9

Table 6 – Ablation of our proposed Iterative Text Decoding Network. "add" and "mul" indicate the cases where our refinement function is replaced by add and multiplication based refinement function respectively. "w/o reference" indicates that Fourier descriptor is not used as the reference location for the Multi-Scale Deformable Attention Module. "w/o refinement" indicates the case where the refinement module is removed.

\mathcal{L}_{SD}	\mathcal{L}_{FD}	\mathcal{L}_{bbox}	CTW1500			MSRA-TD500		
			R(%)	P(%)	F(%)	R(%)	P(%)	F(%)
	✓	✓	75.3	84.4	79.6	56.7	59.9	58.3
✓	✓		82.6	86.5	84.5	82.0	83.5	82.7
✓		✓	81.8	86.2	84.0	81.6	84.2	82.9
✓	✓	✓	82.5	86.9	84.6	79.2	88.3	83.5

Table 7 – Ablation of the loss functions.

\mathcal{L}_{FD} or \mathcal{L}_{bbox} in the matching cost calculation process and loss calculation process reduce the F-measure performance of the proposed FANet by 5.0%, 0.6% and 0.1% on CTW1500 respectively, and by 25.2%, 0.6% and 0.8% on MSRA-TD500 respectively. From this result, we can know that L1 loss for the resampled points of the text contour is more important than other two losses. Nevertheless, mixing the three losses submit the best performance, which indicates that the gains brought by the three losses are not completely overlapping. In order to achieve the best performance, we take the mixed loss of the three losses as the loss function of the proposed FANet.

Dense matching strategy. As shown in Table 2, with only 30 epochs of training, the Dense Matching Strategy (DMS) can bring improvements of 3.3%, 8.6%, 3.5% and 2.9% based on F-measure on ICDAR2015, MSRA-TD500, CTW1500 and TotalText respectively. We attribute this to the fact that DMS can alleviate the overfitting problem caused by lack of positive samples. As the number of epochs increases, the gain brought by DMS becomes smaller, especially on CTW1500 and TotalText. We at-

tribute this to the fact that as the number of training epochs increases, data enhancement can alleviate the performance degradation caused by overfitting and narrows the performance gap between HMS and DMS. So when we are faced with scenarios that enough training epochs are provided such as pre-training, using the original HMS or use DMS with small H_m instead is a better choice. Match number N_m in DMS is an important hyperparameter, compared with the case when $N_m = 1$, setting N_m to 10 will bring relative gain of 3.8% (87.3%vs.83.5%) based on F-measure on MSRA-TD500, which shows the effectiveness of the DMS. Compared with the case when $N_m = 10$, setting N_m to 5 or 15 will reduce the performance of our network by 1.4% (87.3%vs.85.9%) and 1.2% (87.3%vs.86.1%) in F-measure respectively, which indicates that too large or too small N_m will damage the performance of the network. Compared with the case when $N_m = 1$, setting N_m to 3 will bring relative gain of 1.2% (84.7%vs.83.5%), 0.3% (84.9%vs.84.6%) and 0.2% (84.8%vs.84.6%) in F-measure on ICDAR2015, CTW1500 and TotalText respectively. Same as MSRA-TD500, too large or too small N_m will damage the performance of the network. As we can see in Table 5, the optimal choice of match number is 10 on MSRA-TD500 and 3 on ICDAR2015, CTW1500 and TotalText. We can deduce that for a dataset with only a small number of text instances in each image like MSRA-TD500, the problem of overfitting is exacerbated by the lack of positive samples, so a larger N_m can bring the network considerable performance gain, but for datasets with dense text instances in each image like ICDAR2015, CTW1500 and TotalText, a smaller N_m is more appropriate.

5. Conclusion

This paper focus on the fast localization learning and accurate detection for scene text detection. We propose FANet, a Fast convergence and Accurate scene text detection Network, which can achieve the SOTA performance on ICDAR2015, MSRA-TD500, CTW1500 and TotalText. More importantly, FANet can accurately detect scene text of arbitrary shapes with fewer training epochs.

A. Fourier Descriptor Normalization

Theorem 1. *If $\mathcal{Z}(t) = \mathcal{X}(t) + i\mathcal{Y}(t)$ is a univariate continuous periodic function about independent variable t , satisfying $t \in [0, 1]$, the period is 1, $(\mathcal{X}(t), \mathcal{Y}(t)) \in [0, 1]^2$. Then we have the following conclusions:*

$$c_k = \int_0^1 \mathcal{Z}(t)e^{-2\pi ikt} dt, k \in \mathbb{Z} \quad (16)$$

$$c_0 = u_0 + iv_0, u_0, v_0 \in [0, 1] \quad (17)$$

$$c_l = u_l + iv_l, u_l, v_l \in [-\frac{2}{\pi}, \frac{2}{\pi}], l \in \mathbb{Z}, l \neq 0 \quad (18)$$

Proof.

$$\begin{aligned} c_k &= \int_0^1 \mathcal{Z}(t)e^{-2\pi ikt} dt \\ &= \int_0^1 [\mathcal{X}(t) + i\mathcal{Y}(t)][\cos(-2\pi kt) + i\sin(-2\pi kt)]dt \\ &= \int_0^1 [\mathcal{X}(t)\cos(2\pi kt) + \mathcal{Y}(t)\sin(2\pi kt)]dt \\ &\quad + i \int_0^1 [-\mathcal{X}(t)\sin(2\pi kt) + \mathcal{Y}(t)\cos(2\pi kt)]dt \\ &= u_k + iv_k \end{aligned} \quad (19)$$

When $k = 0$, there are the following conclusions:

$$u_0 = \int_0^1 \mathcal{X}(t)dt \in [0, 1] \quad (20)$$

$$v_0 = \int_0^1 \mathcal{Y}(t)dt \in [0, 1] \quad (21)$$

When $k \neq 0$, there are the following conclusions:

$$\begin{aligned} |u_k| &= \left| \int_0^1 [\mathcal{X}(t)\cos(2\pi kt) + \mathcal{Y}(t)\sin(2\pi kt)]dt \right| \\ &\leq \left| \int_0^1 \mathcal{X}(t)\cos(2\pi kt)dt \right| + \left| \int_0^1 \mathcal{Y}(t)\sin(2\pi kt)dt \right| \end{aligned} \quad (23)$$

For term $\int_0^1 \mathcal{X}(t)\cos(2\pi kt)dt$, there are the following in-

equalities:

$$\begin{aligned} -\frac{1}{\pi} &= \int_0^1 \cos(2\pi kt)I[\cos(2\pi kt) < 0]dt \\ &\leq \int_0^1 \mathcal{X}(t)\cos(2\pi kt)I[\cos(2\pi kt) < 0]dt \\ &\leq \int_0^1 \mathcal{X}(t)\cos(2\pi kt)dt \\ &\leq \int_0^1 \mathcal{X}(t)\cos(2\pi kt)I[\cos(2\pi kt) > 0]dt \\ &\leq \int_0^1 \cos(2\pi kt)I[\cos(2\pi kt) > 0]dt \\ &= \frac{4k}{2} \left| \int_0^{\frac{1}{4k}} \cos(2\pi kt)dt \right| \\ &= \frac{4k}{2} \left| \frac{1}{2\pi k} \sin(2\pi kt) \Big|_{t=\frac{1}{4k}} \right| = \frac{1}{\pi} \end{aligned} \quad (24)$$

We can get $|\int_0^1 \mathcal{X}(t)\cos(2\pi kt)dt| \leq \frac{1}{\pi}$, and we can easily prove it in the same way that $|\int_0^1 \mathcal{Y}(t)\sin(2\pi kt)dt| \leq \frac{1}{\pi}$. We substitute it into Eq 23, then we can get:

$$|u_k| \leq \frac{1}{\pi} + \frac{1}{\pi} = \frac{2}{\pi}, k \in \mathbb{Z}, k \neq 0 \quad (25)$$

In the same way, we can easily prove that:

$$|v_k| \leq \frac{2}{\pi}, k \in \mathbb{Z}, k \neq 0 \quad (26)$$

□

B. Fourier descriptor as the reference location

Let $\{\mathbf{x}^l\}_{l=1}^L$ be the input multi-scale feature maps, where $\mathbf{x}^l \in \mathbb{R}^{C \times H_l \times W_l}$. Let $\hat{\mathbf{p}}_q \in [0, 1]^2$ be the normalized coordinates of the reference point for each query element q , then the Multi-Scale Deformable Attention module [37] is applied as Equation 22,

where m indexes the attention head, l indexes the input feature level, and k indexes the sampling point. $\Delta \mathbf{p}_{qmls}$ and A_{qmls} denote the sampling offset and attention weight of the s -th sampling point in the l -th feature level and the m -th attention head, respectively. The scalar attention weight A_{qmls} is normalized by $\sum_{l=1}^L \sum_{s=1}^S A_{qmls} = 1$. Here, we use normalized coordinates $\hat{\mathbf{p}}_q \in [0, 1]^2$ for the clarity of scale formulation, in which the normalized coordinates $(0, 0)$ and $(1, 1)$ indicate the top-left and the bottom-right image corners, respectively. Function $\phi_l(\hat{\mathbf{p}}_q)$ in Equation 22 rescales the normalized coordinates $\hat{\mathbf{p}}_q$ to the input feature map of the l -th level. The multi-scale deformable attention samples LS points from multi-scale feature maps. In the proposed FANet, we consider the calculation process of for query q in d -th transformer decoder layer. We

$$\text{MSDeformAttn}(z_q, \hat{\mathbf{p}}_q, \{\mathbf{x}^l\}_{l=1}^L) = \sum_{m=1}^M \mathbf{W}_m \left[\sum_{l=1}^L \sum_{s=1}^S A_{qm\ell s} \cdot \mathbf{W}'_m \mathbf{x}^l (\phi_l(\hat{\mathbf{p}}_q) + \Delta \mathbf{p}_{qm\ell s}) \right] \quad (22)$$

first obtain the normalized Fourier descriptor predicted by the $(d-1)$ -th decoder layer of query q , which we denote as $\mathbf{c} = [u_{-K}, v_{-K}, \dots, u_0, v_0, \dots, u_K, v_K] \in \mathbb{R}^{2(2K+1)}$. We then calculate the normalized coordinate points on the predict text contour in spatial domain by Inverse Discrete Fourier Transform (IDFT):

$$\mathbf{p}_{qn} = \mathcal{F}^{-1}\left(\frac{n}{N}, \mathbf{c}\right), n = 1, \dots, N \quad (27)$$

where $\mathbf{p}_{qn} = (x_{qn}, y_{qn})$ is the n -th point on the text contour predicted by query q , \mathcal{F}^{-1} is the Inverse Fourier Transform (IFT) function, N is the sampling number on the text contour. We then calculate the bounding box of the text contour:

$$x_q = E_i(x_{qn}) \quad (28)$$

$$y_q = E_i(y_{qn}) \quad (29)$$

$$w_q = \max_i(x_{qn}) - \min_i(x_{qn}) \quad (30)$$

$$h_q = \max_i(y_{qn}) - \min_i(y_{qn}) \quad (31)$$

Where $\{x_q, y_q, w_q, h_q\}$ is the bounding box of the text contour. We use $\phi_l((x_q, y_q))$ instead of $\phi_l(\hat{\mathbf{p}}_q)$ as the new reference point for query q . The sampling offset $\Delta \mathbf{p}_{m\ell qh}$ is also modulated by the box size, as $(\Delta \mathbf{p}_{qm\ell s x} w_q, \Delta \mathbf{p}_{qm\ell s y} h_q)$.

C. Refinement function

Theorem 2. *If $y = f[x + f^{-1}(x_0)]$ is a continuous function about x , where f is a differentiable function and $x_0 \in \mathbb{R}$ is a constant value, then:*

$$\lim_{x \rightarrow 0} \frac{\partial y}{\partial x} = \frac{\partial f(z)}{\partial z} \Big|_{z=f^{-1}(x_0)} \quad (32)$$

Proof.

$$\begin{aligned} \lim_{x \rightarrow 0} \frac{\partial y}{\partial x} &= \lim_{x \rightarrow 0} \frac{\partial f(z)}{\partial z} \Big|_{z=x+f^{-1}(x_0)} \\ &= \frac{\partial f(z)}{\partial z} \Big|_{z=f^{-1}(x_0)} \end{aligned} \quad (33)$$

□

Theorem 3. *If $y = f[e^x f^{-1}(x_0)]$ is a continuous function about x , where f is a differentiable function and $x_0 \in \mathbb{R}$ is a constant value, then:*

$$\lim_{x \rightarrow 0} \frac{\partial y}{\partial x} = \frac{\partial f(z)}{\partial z} \Big|_{z=f^{-1}(x_0)} f^{-1}(x_0) \quad (34)$$

Proof.

$$\begin{aligned} \lim_{x \rightarrow 0} \frac{\partial y}{\partial x} &= \lim_{x \rightarrow 0} \frac{\partial f(z)}{\partial z} \Big|_{z=e^x f^{-1}(x_0)} f^{-1}(x_0) e^x \\ &= \frac{\partial f(z)}{\partial z} \Big|_{z=f^{-1}(x_0)} f^{-1}(x_0) \end{aligned} \quad (35)$$

□

References

- [1] Nicolas Carion, Francisco Massa, Gabriel Synnaeve, Nicolas Usunier, Alexander Kirillov, and Sergey Zagoruyko. End-to-end object detection with transformers. In Andrea Vedaldi, Horst Bischof, Thomas Brox, and Jan-Michael Frahm, editors, *Computer Vision - ECCV 2020 - 16th European Conference, Glasgow, UK, August 23-28, 2020, Proceedings, Part I*, volume 12346 of *Lecture Notes in Computer Science*, pages 213–229. Springer, 2020.
- [2] Chee Kheng Chng and Chee Seng Chan. Total-text: A comprehensive dataset for scene text detection and recognition. In *14th IAPR International Conference on Document Analysis and Recognition, ICDAR 2017, Kyoto, Japan, November 9-15, 2017*, pages 935–942. IEEE, 2017.
- [3] Jifeng Dai, Haozhi Qi, Yuwen Xiong, Yi Li, Guodong Zhang, Han Hu, and Yichen Wei. Deformable convolutional networks. In *IEEE International Conference on Computer Vision, ICCV 2017, Venice, Italy, October 22-29, 2017*, pages 764–773. IEEE Computer Society, 2017.
- [4] Pengwen Dai, Sanyi Zhang, Hua Zhang, and Xiaochun Cao. Progressive contour regression for arbitrary-shape scene text detection. In *IEEE Conference on Computer Vision and Pattern Recognition, CVPR 2021, virtual, June 19-25, 2021*, pages 7393–7402. Computer Vision Foundation / IEEE, 2021.
- [5] Jia Deng, Wei Dong, Richard Socher, Li-Jia Li, Kai Li, and Li Fei-Fei. Imagenet: A large-scale hierarchical image database. In *2009 IEEE Computer Society Conference on Computer Vision and Pattern Recognition (CVPR 2009), 20-25 June 2009, Miami, Florida, USA*, pages 248–255. IEEE Computer Society, 2009.
- [6] Jacob Devlin, Ming-Wei Chang, Kenton Lee, and Kristina Toutanova. BERT: pre-training of deep bidirectional transformers for language understanding. In Jill Burstein, Christy Doran, and Thamar Solorio, editors, *Proceedings of the 2019 Conference of the North American Chapter of the Association for Computational Linguistics: Human Language Technologies, NAACL-HLT 2019, Minneapolis, MN, USA, June 2-7, 2019, Volume 1 (Long and Short Papers)*, pages 4171–4186. Association for Computational Linguistics, 2019.
- [7] Alexey Dosovitskiy, Lucas Beyer, Alexander Kolesnikov, Dirk Weissenborn, Xiaohua Zhai, Thomas Unterthiner,

- Mostafa Dehghani, Matthias Minderer, Georg Heigold, Sylvain Gelly, Jakob Uszkoreit, and Neil Houlsby. An image is worth 16x16 words: Transformers for image recognition at scale. In *9th International Conference on Learning Representations, ICLR 2021, Virtual Event, Austria, May 3-7, 2021*. OpenReview.net, 2021.
- [8] Kaiming He, Georgia Gkioxari, Piotr Dollár, and Ross B. Girshick. Mask R-CNN. In *ICCV*, pages 2980–2988, 2017.
- [9] Kaiming He, Xiangyu Zhang, Shaoqing Ren, and Jian Sun. Deep residual learning for image recognition. In *2016 IEEE Conference on Computer Vision and Pattern Recognition, CVPR 2016, Las Vegas, NV, USA, June 27-30, 2016*, pages 770–778. IEEE Computer Society, 2016.
- [10] Dimosthenis Karatzas, Lluís Gomez-Bigorda, Angelos Nicolaou, Suman K. Ghosh, Andrew D. Bagdanov, Masakazu Iwamura, Jiri Matas, Lukas Neumann, Vijay Ramaseshan Chandrasekhar, Shijian Lu, Faisal Shafait, Seichi Uchida, and Ernest Valveny. ICDAR 2015 competition on robust reading. In *13th International Conference on Document Analysis and Recognition, ICDAR 2015, Nancy, France, August 23-26, 2015*, pages 1156–1160. IEEE Computer Society, 2015.
- [11] Zhanghui Kuang, Hongbin Sun, Zhizhong Li, Xiaoyu Yue, Tsui Hin Lin, Jianyong Chen, Huaqiang Wei, Yiqin Zhu, Tong Gao, Wenwei Zhang, Kai Chen, Wayne Zhang, and Dahua Lin. MMOCR: A comprehensive toolbox for text detection, recognition and understanding. In Heng Tao Shen, Yueting Zhuang, John R. Smith, Yang Yang, Pablo Cesar, Florian Metze, and Balakrishnan Prabhakaran, editors, *MM '21: ACM Multimedia Conference, Virtual Event, China, October 20 - 24, 2021*, pages 3791–3794. ACM, 2021.
- [12] Minghui Liao, Zhaoyi Wan, Cong Yao, Kai Chen, and Xiang Bai. Real-time scene text detection with differentiable binarization. In *The Thirty-Fourth AAAI Conference on Artificial Intelligence, AAAI 2020, The Thirty-Second Innovative Applications of Artificial Intelligence Conference, IAAI 2020, The Tenth AAAI Symposium on Educational Advances in Artificial Intelligence, EAAI 2020, New York, NY, USA, February 7-12, 2020*, pages 11474–11481. AAAI Press, 2020.
- [13] Tsung-Yi Lin, Priya Goyal, Ross B. Girshick, Kaiming He, and Piotr Dollár. Focal loss for dense object detection. In *IEEE International Conference on Computer Vision, ICCV 2017, Venice, Italy, October 22-29, 2017*, pages 2999–3007. IEEE Computer Society, 2017.
- [14] Xiyang Liu, Gaofeng Meng, and Chunhong Pan. Scene text detection and recognition with advances in deep learning: a survey. *Int. J. Document Anal. Recognit.*, 22(2):143–162, 2019.
- [15] Yuliang Liu, Hao Chen, Chunhua Shen, Tong He, Lianwen Jin, and Liangwei Wang. Abcnet: Real-time scene text spotting with adaptive bezier-curve network. In *2020 IEEE/CVF Conference on Computer Vision and Pattern Recognition, CVPR 2020, Seattle, WA, USA, June 13-19, 2020*, pages 9806–9815. Computer Vision Foundation / IEEE, 2020.
- [16] Yuliang Liu, Lianwen Jin, Shuaitao Zhang, Canjie Luo, and Sheng Zhang. Curved scene text detection via transverse and longitudinal sequence connection. *Pattern Recognit.*, 90:337–345, 2019.
- [17] Shangbang Long, Jiaqiang Ruan, Wenjie Zhang, Xin He, Wenhao Wu, and Cong Yao. Textsnake: A flexible representation for detecting text of arbitrary shapes. In Vittorio Ferrari, Martial Hebert, Cristian Sminchisescu, and Yair Weiss, editors, *Computer Vision - ECCV 2018 - 15th European Conference, Munich, Germany, September 8-14, 2018, Proceedings, Part II*, volume 11206 of *Lecture Notes in Computer Science*, pages 19–35. Springer, 2018.
- [18] Zobeir Raisi, Mohamed A. Naiel, Georges Younes, Steven Wardell, and John S. Zelek. Transformer-based text detection in the wild. In *IEEE Conference on Computer Vision and Pattern Recognition Workshops, CVPR Workshops 2021, virtual, June 19-25, 2021*, pages 3162–3171. Computer Vision Foundation / IEEE, 2021.
- [19] Hamid Rezaatofghi, Nathan Tsoi, JunYoung Gwak, Amir Sadeghian, Ian D. Reid, and Silvio Savarese. Generalized intersection over union: A metric and a loss for bounding box regression. In *IEEE Conference on Computer Vision and Pattern Recognition, CVPR 2019, Long Beach, CA, USA, June 16-20, 2019*, pages 658–666. Computer Vision Foundation / IEEE, 2019.
- [20] Karen Simonyan and Andrew Zisserman. Very deep convolutional networks for large-scale image recognition. In Yoshua Bengio and Yann LeCun, editors, *3rd International Conference on Learning Representations, ICLR 2015, San Diego, CA, USA, May 7-9, 2015, Conference Track Proceedings*, 2015.
- [21] Russell Stewart, Mykhaylo Andriluka, and Andrew Y. Ng. End-to-end people detection in crowded scenes. In *2016 IEEE Conference on Computer Vision and Pattern Recognition, CVPR 2016, Las Vegas, NV, USA, June 27-30, 2016*, pages 2325–2333. IEEE Computer Society, 2016.
- [22] Ashish Vaswani, Noam Shazeer, Niki Parmar, Jakob Uszkoreit, Llion Jones, Aidan N. Gomez, Lukasz Kaiser, and Illia Polosukhin. Attention is all you need. In Isabelle Guyon, Ulrike von Luxburg, Samy Bengio, Hanna M. Wallach, Rob Fergus, S. V. N. Vishwanathan, and Roman Garnett, editors, *Advances in Neural Information Processing Systems 30: Annual Conference on Neural Information Processing Systems 2017, December 4-9, 2017, Long Beach, CA, USA*, pages 5998–6008, 2017.
- [23] Andreas Veit, Tomas Matera, Lukas Neumann, Jiri Matas, and Serge Belongie. Coco-text: Dataset and benchmark for text detection and recognition in natural images. In *arXiv preprint arXiv:1601.07140*, 2016.
- [24] Fangfang Wang, Yifeng Chen, Fei Wu, and Xi Li. Text-tray: Contour-based geometric modeling for arbitrary-shaped scene text detection. In Chang Wen Chen, Rita Cucchiara, Xian-Sheng Hua, Guo-Jun Qi, Elisa Ricci, Zhengyou Zhang, and Roger Zimmermann, editors, *MM '20: The 28th ACM International Conference on Multimedia, Virtual Event / Seattle, WA, USA, October 12-16, 2020*, pages 111–119. ACM, 2020.
- [25] Wenhao Wang, Enze Xie, Xiang Li, Wenbo Hou, Tong Lu, Gang Yu, and Shuai Shao. Shape robust text detection with progressive scale expansion network. In *IEEE Conference on Computer Vision and Pattern Recognition, CVPR 2019*,

- Long Beach, CA, USA, June 16-20, 2019, pages 9336–9345. Computer Vision Foundation / IEEE, 2019.
- [26] Wenhai Wang, Enze Xie, Xiaoge Song, Yuhang Zang, Wenjia Wang, Tong Lu, Gang Yu, and Chunhua Shen. Efficient and accurate arbitrary-shaped text detection with pixel aggregation network. In *2019 IEEE/CVF International Conference on Computer Vision, ICCV 2019, Seoul, Korea (South), October 27 - November 2, 2019*, pages 8439–8448. IEEE, 2019.
- [27] Weijia Wu, Yuanqiang Cai, Debing Zhang, Sibao Wang, Zhuang Li, Jiahong Li, Yejun Tang, and Hong Zhou. A bilingual, openworld video text dataset and end-to-end video text spotter with transformer. *arXiv preprint arXiv:2112.04888*, 2021.
- [28] Weijia Wu, Ning Lu, Enze Xie, Yuxing Wang, Wenwen Yu, Cheng Yang, and Hong Zhou. Synthetic-to-real unsupervised domain adaptation for scene text detection in the wild. In *Proceedings of the Asian Conference on Computer Vision*, 2020.
- [29] Weijia Wu, Enze Xie, Ruimao Zhang, Wenhai Wang, Guan Pang, Zhen Li, Hong Zhou, and Ping Luo. Selftext beyond polygon: Unconstrained text detection with box supervision and dynamic self-training. *arXiv preprint arXiv:2011.13307*, 2020.
- [30] Weijia Wu, Jici Xing, Cheng Yang, Yuxing Wang, and Hong Zhou. Texts as lines: text detection with weak supervision. *Mathematical Problems in Engineering*, 2020, 2020.
- [31] Weijia Wu, Jici Xing, and Hong Zhou. Textcohesion: Detecting text for arbitrary shapes. *arXiv preprint arXiv:1904.12640*, 2019.
- [32] Weijia Wu, Debing Zhang, Ying Fu, Chunhua Shen, Hong Zhou, Yuanqiang Cai, and Ping Luo. End-to-end video text spotting with transformer. *arXiv preprint arXiv:2203.10539*, 2022.
- [33] Cong Yao, Xiang Bai, Wenyu Liu, Yi Ma, and Zhuowen Tu. Detecting texts of arbitrary orientations in natural images. In *2012 IEEE Conference on Computer Vision and Pattern Recognition, Providence, RI, USA, June 16-21, 2012*, pages 1083–1090. IEEE Computer Society, 2012.
- [34] Qixiang Ye and David S. Doermann. Text detection and recognition in imagery: A survey. *IEEE Trans. Pattern Anal. Mach. Intell.*, 37(7):1480–1500, 2015.
- [35] Shi-Xue Zhang, Xiaobin Zhu, Jie-Bo Hou, Chang Liu, Chun Yang, Hongfa Wang, and Xu-Cheng Yin. Deep relational reasoning graph network for arbitrary shape text detection. In *CVPR, CVPR 2020, Seattle, WA, USA, June 13-19, 2020*, pages 9696–9705, 2020.
- [36] Yu Zhou, Hongtao Xie, Shancheng Fang, Yan Li, and Yongdong Zhang. Crnet: A center-aware representation for detecting text of arbitrary shapes. In *MM '20: The 28th ACM International Conference on Multimedia, Virtual Event / Seattle, WA, USA, October 12-16, 2020*, pages 2571–2580. ACM, 2020.
- [37] Xizhou Zhu, Weijie Su, Lewei Lu, Bin Li, Xiaogang Wang, and Jifeng Dai. Deformable DETR: deformable transformers for end-to-end object detection. In *9th International Conference on Learning Representations, ICLR 2021, Virtual Event, Austria, May 3-7, 2021*. OpenReview.net, 2021.
- [38] Yiqin Zhu, Jianyong Chen, Lingyu Liang, Zhanghui Kuang, Lianwen Jin, and Wayne Zhang. Fourier contour embedding for arbitrary-shaped text detection. In *IEEE Conference on Computer Vision and Pattern Recognition, CVPR 2021, virtual, June 19-25, 2021*, pages 3123–3131. Computer Vision Foundation / IEEE, 2021.
- [39] Yingying Zhu, Cong Yao, and Xiang Bai. Scene text detection and recognition: recent advances and future trends. *Frontiers Comput. Sci.*, 10(1):19–36, 2016.